Journal of Medicinal Chemistry

Article

pubs.acs.org/jmc

Identification of Clinically Viable Quinolinol Inhibitors of Botulinum Neurotoxin A Light Chain

Dejan Caglič,[†] Michelle C. Krutein,[†] Kristin M. Bompiani,[†] Deborah J. Barlow,[‡] Galit Benoni,[†] Jeffrey C. Pelletier,[§] Allen B. Reitz,[§] Luke L. Lairson,[†] Karen L. Houseknecht,[‡] Garry R. Smith,[§] and Tobin J. Dickerson*[,†]

[†]Department of Chemistry, The Scripps Research Institute, 10550 North Torrey Pines Road, La Jolla, California 92037, United States

[‡]Department of Pharmaceutical Sciences, University of New England College of Pharmacy, Portland, Maine 04103, United States

[§]Fox Chase Chemical Diversity Center, Doylestown, Pennsylvania 18902, United States

Supporting Information

ABSTRACT: Botulinum neurotoxins (BoNT) are the most potent toxins known and a significant bioterrorist threat. Few small molecule compounds have been identified that are active in cell-based or animal models, potentially due to toxin enzyme plasticity. Here we screened commercially available quinolinols, as well as synthesized hydroxyquinolines. Seventy-two compounds had IC_{50} values below 10 μM, with the best compound exhibiting submicromolar inhibition (IC_{50} = 0.8 μM). Structure−activity relationship trends showed that the enzyme tolerates various substitutions at R_1 but has a clear preference for bulky aryl amide groups at R_2, while methylation at R_3 increased inhibitor potency. Evaluation of the most potent compounds in an ADME panel showed that these compounds possess poor solubility at pH 6.8, but display excellent solubility at low pH, suggesting that oral dosing may be possible. Our data show the potential of quinolinol compounds as BoNT therapeutics due to their good in vitro potencies and favorable ADME properties.

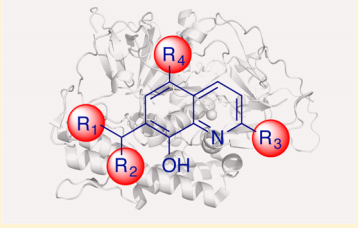

INTRODUCTION

Clostridium botulinum neurotoxin serotype A (BoNT/A), the most potent toxin known to man ($LD_{50} \approx 0.5$ ng/kg[1]), disrupts neurotransmission by cleaving proteins involved in the exocytosis of the neurotransmitter acetylcholine from motor neurons at the neuromuscular junction. Inhibition of acetylcholine release, in turn, results in flaccid paralysis and may lead to host death due to heart or respiratory failure. Because of its extraordinary toxicity and ease of production in large quantities, BoNT/A is considered a potential bioterrorism weapon.[2]

The mechanism of action of BoNT includes binding to motor neuron surface receptors, cellular uptake via endocytosis, and escape of the N-terminal catalytic domain from endosomes into the cytosol. Once in the cytosol, the BoNT/A light chain (BoNT/A LC), a zinc-dependent metalloprotease, cleaves its cognate protein substrate, SNAP-25 (Synaptosomal Associated Protein of 25 kDa). SNAP-25 is a member of the SNARE (Soluble NSF Attachment Protein Receptor) complex of proteins involved in acetylcholine exocytosis. Cleavage of SNAP-25 disrupts acetylcholine neurotransmission from motor neurons to their target muscle cells, ultimately resulting in flaccid paralysis.[3]

Because of the rapid internalization and intracellular site of action of the toxin, treatments that inhibit holotoxin binding and/or internalization, including the only existing treatment of BoNT intoxication with passive immunization with equine or human neutralizing antibodies, have a limited window of application and become inefficient once the toxin is internalized into the target neuronal cell. However, compounds that target intracellular BoNT/A LC activity have a much larger window of application due to the extremely long half-life of the BoNT/A LC. Therefore, we and others have focused primarily on targeting BoNT/A LC enzymatic activity and have reported a number of small molecule inhibitors of BoNT/A LC that are highly efficient in vitro, but when used ex vivo or in vivo, most of these compounds fail because of their poor pharmacokinetic properties.[4,5] Consequently, there is a great demand to identify and develop new inhibitors of BoNT/A LC with improved in vivo properties that would not only show good in vitro inhibition of the isolated toxin but could also reverse symptoms of botulism in an intoxicated host.

Most reported inhibitors of BoNT/A LC share a common motif, that is, a Zn^{2+} chelator that prevents water-catalyzed proteolysis of the peptide bond of the protein substrate SNAP-25. One such chelator is the hydroxamate moiety used in BoNT/A LC inhibitors developed by our laboratory and others.[4−6] Although hydroxamate-based inhibitors were shown to exhibit excellent in vitro potency against the recombinant enzyme with K_i in the nanomolar range (K_i of one of the most potent hydroxamate compounds to date, (2*E*)-3-(3-chloro-6-fluoro-benzo[b]thiophen-2-yl)-*N*-hydroxy-(*E*)-acrylamide, is 77 nM),[4] these compounds generally suffer from poor bioavailability, short metabolic half-lives that seldom exceed one hour,[4] and high cytotoxicity.[5] In addition, we have recently reexamined a series of hydroxamate inhibitors and found an

Received: August 8, 2013
Published: January 5, 2014

   dx.doi.org/10.1021/jm4012164 | *J. Med. Chem.* 2014, 57, 669−676

inconsistency in structure−activity relationship (SAR) trends across similar hydroxamate compounds, suggesting a relative plasticity of the BoNT/A LC active site and cautioning against making generalizations across compound series.[7] Quinolinol compounds have been reported as an alternative class of BoNT/A LC inhibitors and were shown to have good ex vivo properties in cell-based, as well as tissue-based, assays.[8] However, SAR for this series of compounds and further pharmacokinetic data have not been reported. In light of the light chain active site plasticity, we examined the SAR of BoNT/A LC quinolinol inhibitors and assessed the pharmacologic parameters of the best inhibitors in ADME studies.

RESULTS AND DISCUSSION

Traditional approaches for the discovery and development of BoNT/A LC inhibitors have been based on screening efforts to obtain novel chemotypes that target the catalytic activity of the LC metalloprotease. Although such approaches generally result in compounds with improved in vitro potency compared to existing inhibitors, these compounds have displayed poor efficacy when advanced into cellular models, presumably due to various limitations including low aqueous solubility and poor cell permeability. In addition, these compounds were shown to suffer from disappointing pharmacokinetic properties (e.g., half-life < 1 h) when tested in animal models (T.J.D. and K.L.H., unpublished data). Furthermore, our recent analysis of the SAR present in the cinnamyl hydroxamate inhibitor series has demonstrated that crystal structure-guided optimization of BoNT/A LC inhibitors can overlook compounds with greater potency than the parent lead.[7] In this case, optimized molecules experimentally found to have increased potencies were predicted to be poor inhibitors that were unable to fit into the active site.

We hypothesized that enzyme flexibility of the BoNT/A LC might have resulted in a similar phenomenon in other inhibitor series; to test this, we analyzed the quinolinol series of inhibitors. The quinolinol moiety is a known chelating motif and therefore represents a viable moiety for a metalloproteinase inhibitor. Quinolinol inhibitors (Figure 1) have been modeled

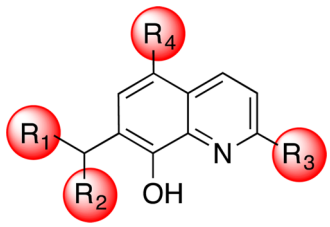

Figure 1. General structure of 8-hydroxy-quinoline compounds that are potent BoNT/A LC inhibitors. Substitutions investigated in the study are numbered R_1 through R_4 in shaded circles.

to bind into the active site of BoNT/A LC with specific contacts formed between the catalytic zinc as well as surrounding active site residues,[9] similar to what was initially proposed for the hydroxamate class of inhibitors.[10]

A range of quinolinol compounds are commercially available from ChemDiv and ChemBridge small molecule repositories and were included into a screening set based on the following criteria: (a) the compounds would have desirable drug-like properties, such as hydrophilicity, low molecular weight, favorable number of hydrogen bond acceptors and donors; (b) the compounds were amenable to structural modifications in order to optimize activity while still retaining drug-like properties; (c) the compounds would essentially be devoid of potentially reactive or known problematic moieties including aldehydes, ketones, charged compounds, and carboxylic and sulfonic acids.

The inhibitory activity of the quinolinol compounds was tested in the SNAPtide assay, an established assay for identification of BoNT/A LC inhibitors.[11] The assay measures changes in fluorescence produced by cleavage of a fluorogenic substrate that consists of a synthetic peptide derived from the amino acid sequence of SNAP-25 flanking the natural BoNT/A LC cleavage site as well as a fluorophore/quencher pair. This assay is a useful primary screen for BoNT/A inhibitor screening campaigns because of its simplicity, automation potential, and ability to screen numerous compounds simultaneously.[5] However, the assay cannot be utilized to determine more rigorous kinetic constants, such as the K_i. Because the K_M of the SNAPtide substrate is well above 1 mM, any assay with this substrate is performed under substrate-limiting conditions.[12]

One hundred eighty-eight commercially available quinolinol derivatives were initially screened at a final concentration of 10 μM. Interestingly, more than half of the compounds tested (54% hit rate) exhibited greater than 50% inhibition of BoNT/A LC activity toward the SNAPtide substrate, implying the enzyme can tolerate various substitutions of the main quinolinol scaffold and suggesting significant plasticity of the active site cleft. The Z'-factor, a measure of statistical predictability of results obtained by a high-throughput method, of our primary screen was 0.92, where a Z'-factor between 0.5 and 1.0 signifies a screening assay with excellent quality.[13]

Subsequently, a secondary follow-up screen was performed on a subset of 90 compounds, including 25 compounds identified in the primary screen as less potent (i.e., <50% inhibition) or inactive. Using this assay, IC_{50} values were determined for all 90 active compounds (Table 1 and Supplemental Table 1). Of this set, 80% of the compounds showed IC_{50} values <10 μM, with the best compounds exhibiting submicromolar IC_{50}. Seven compounds that exhibited between 25% and 50% inhibition in the primary screen at 10 μM, were shown to have IC_{50} values <10 μM, resulting in a false-negative discovery rate of the primary screen of 7.8%. The IC_{50} of compound **4**, the most potent compound in the library, was 0.8 ± 0.1 μM.

Despite the promiscuity of the enzyme for various substitutions on the main quinolinol backbone (Figure 1), some structure−activity relationships could be deducted from the inhibitory data (Table 1). Compounds with a five- or six-membered heterocycle at both R_1 and R_2 showed good inhibition, and compounds that did not have a 6-membered heterocycle at R_2 had severely decreased inhibitory activity (**1**−**3**, **15**, **22**, **27**−**29**). The enzyme tolerated virtually any substitution on the R_1 heterocycle, including electron donating (**4**−**12**) and electron withdrawing (**15**−**37**) groups on the R_1 phenyl ring; moreover, substitutions of the R_1 phenyl ring with heterocyclic pyridyl (**40**−**53**) were tolerated. In addition, a heterocyclic pyridine-3-yl ring at the R_1 position (**41**, **43**, **45**, **47**, **49**, **51**, **53**) was favored over the pyridine-2-yl substitution (**40**, **42**, **44**, **46**, **48**, **50**, **52**) with the pyridine-3-yl compounds being up to 60% more potent (Table 1), suggesting that 3-N atom of the pyridine ring forms favorable interactions with the side chains of LC active site residues. Presumably, this interaction is with Arg363, which has been reported to interact with the R_2 moiety of quinolinol inhibitors based on molecular

dx.doi.org/10.1021/jm4012164 | J. Med. Chem. 2014, 57, 669−676

Table 1. Inhibitory Activities of 8-Hydroxy-quinolines toward BoNT/A LC

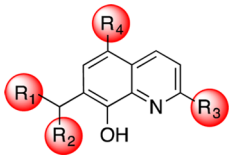

Compound	Chembridge or ChemDiv ID	R_1	R_2	R_3	R_4	IC_{50} (μM)
1	5924147			H	H	>100
2	5925700			H	H	>100
3	5928516			H	H	>100
4	5838194			H	H	0.8 ± 0.1
5	6633702			H	H	3.6 ± 0.3
6	6637624			CH_3	H	1.6 ± 0.1
7	6377743			CH_3	H	10.7 ± 1.1
8	7630436			CH_3	H	0.9 ± 0.1
9	6377946			H	H	13.4 ± 0.3
10	7330066			CH_3	H	2.1 ± 0.3
11	6381500			H	H	4.6 ± 0.3
12	7633631			CH_3	H	1.1 ± 0.2
13	6381368			CH_3	H	1.4 ± 0.1
14	6636291			CH_3	H	3.5 ± 0.6
15	5845249			H	H	>100
16	6380954			H	H	3.3 ± 0.3
17	7633962			CH_3	H	2.0 ± 0.2
18	7629244			H	H	1.5 ± 0.2
19	7319416			CH_3	H	1.2 ± 0.1
20	6376791			H	H	6.2 ± 0.5
21	6635878			CH_3	H	3.0 ± 0.2
22	5924214			H	H	>100
23	6379137			H	H	7.1 ± 0.4
24	6378600			CH_3	H	2.8 ± 0.2
25	6372490			H	H	2.5 ± 0.2
26	6637173			CH_3	H	2.1 ± 0.2
27	5848587			H	H	>100
28	5926670			H	H	>100

Compound	Chembridge or ChemDiv ID	R_1	R_2	R_3	R_4	IC_{50} (μM)
29	5926377			H	H	>100
30	5928396			H	H	7.1 ± 1.2
31	6380808			H	H	3.5 ± 0.4
32	7633178			CH_3	H	2.5 ± 0.3
33	6378687			CH_3	H	4.5 ± 0.7
34	6634547			H	H	4.3 ± 0.4
35	7630693			CH_3	H	1.0 ± 0.1
36	6646208			H	H	5.6 ± 0.4
37	6633429			CH_3	H	1.9 ± 0.3
38	7021092			CH_3	H	2.0 ± 0.2
39	7719526			CH_3	H	>100
40	8397-0126			H	H	5.6 ± 0.8
41	8397-0127			H	H	1.9 ± 0.3
42	8397-0165			H	H	5.1 ± 0.6
43	8397-0166			H	H	2.9 ± 0.4
44	8397-0270			H	H	7.8 ± 1.3
45	8397-0271			H	H	4.2 ± 1.0
46	8397-0298			H	H	5.6 ± 1.3
47	8397-0299			H	H	3.0 ± 0.3
48	8397-0558			H	H	5.1 ± 1.0
49	8397-0559			H	H	4.4 ± 0.3
50	8397-0572			H	H	5.2 ± 0.7
51	8397-0573			H	H	2.3 ± 0.4
52	8397-0664			H	H	16.7 ± 1.9
53	8397-0665			H	H	6.7 ± 1.1

dx.doi.org/10.1021/jm4012164 | J. Med. Chem. 2014, 57, 669−676

docking experiments.[8,9] However, bulky groups such as 3-*O*-benzyl substitution on the R_1 phenyl ring were well tolerated by the enzyme and resulted in inhibitors with good to excellent potencies (IC_{50} values of 1.4 and 3.5 μM for compounds **13** and **14**, respectively). These findings are consistent with our previous observations that the active site of BoNT/A LC is flexible and can efficiently accommodate sterically large moieties not readily predicted from structural data.[7]

Analysis of R_2 substitutions showed unexpected results. When the pyridyl amide at the R_2 position was substituted with short alkyl groups, such as acetamide (**15**, **27**, **28**), propylamide (**1**, **22**, **29**), butylamide (**2**), and isobutylamide (**3**), the compounds became virtually inactive. However, bulky aryl amide substitutions (compounds **4**−**14**, **16**−**21**, **23**−**26**, **30**−**53**) rendered the inhibitors active, suggesting that the R_2 group might interact with an aromatic residue or the zinc cation of BoNT/A LC. An interesting finding came from analyzing compounds **38** and **39**. Both compounds bear a 5-methyl-thiophen-2-yl substitution at the R_1 position, but only compound **38**, with unsubstituted R_2 2-pyridyl ring, resulted in potent inhibition of BoNT/A LC. In contrast, the 6-methyl group on the R_2 ring (**39**) rendered the compound completely inactive, suggesting the methyl group produces a significant steric clash with the walls of the BoNT/A LC binding pocket. However, this trend is not globally true; comparison of compounds **13** and **14** shows that methylation of the R_2 2-pyridyl ring does not result in dramatically reduced inhibition.

The presence or absence of a methyl group at the R_3 position (compound pairs **5**−**6**, **9**−**10**, **11**−**12**, **16**−**17**, **18**−**19**, **20**−**21**, **23**−**24**, **25**−**26**, **31**−**32**, **34**−**35**, **36**−**37**) had a clear effect on the potency of inhibitors, where the presence of a methyl group decreased the IC_{50} values of corresponding inhibitors with otherwise the same structure by as much as 85% (13.4 vs 2.1 μM for compounds **9** and **10**). This suggests that the R_3 methyl group forms favorable interactions with the side chains of the LC active site cleft.

In an attempt to more completely understand which parts of the quinolinol molecule were absolutely required for the inhibition of BoNT/A LC, we conducted additional sub-structure analysis of portions of the parent scaffold and synthesized the required compounds (Table 2). 8-Hydroxy-quinoline (**54**) served as the simplest compound bearing only the quinoline backbone with the chelating motif, but without any additional structural determinants that could facilitate binding of the inhibitor into the active site cleft of the protease and thus increase its potency. As expected, 8-hydroxy-quinoline showed poor inhibition of SNAPtide cleavage at inhibitor concentrations ≤30 μM (Table 2), suggesting the quinoline backbone by itself is not sufficient for efficient inhibition. In addition, when the prototype quinolinol compound (**57**) that bears an aryl group on each of the R_1 and R_2 positions was tested, it exhibited relatively good potency of 2.2 μM, implying that both the R_1 and R_2 substitutions are required for productive docking of the inhibitor into the active site and, consequently, potent inhibition (Table 2). When the R_1 group was removed altogether (**56**), the molecule lost most of its inhibitory activity (IC_{50} = 27 μM), suggesting that the R_1 moiety is needed for either proper molecular conformation or favorable interaction of the inhibitor with BoNT/A LC. Unfortunately, multiple attempts to synthesize an analogous molecule in which R_2 was missing failed, yielding only starting material.

An important finding came from a compound where the 8-hydroxy group of the compound **57** was protected with an isopropyl group (Supplemental Figure 1), rendering the compound completely inactive (IC_{50} >100 μM, data not shown), confirming the necessity of the 8-hydroxy group and suggesting its role in chelation of the catalytic zinc.

Further analysis of the structures of quinolinol inhibitors uncovered a distinct similarity to molecules that have been advanced into clinical testing for indications unrelated to botulism. The compound 8-hydroxy-quinoline (**54**), although not a very potent BoNT/A LC inhibitor, and the 8-hydroxy-quinoline backbone, are structurally related to two clinically approved drugs, clioquinol (**58**; Figure 2) and chloroxine (**60**; Figure 2), both of which possess good pharmacokinetic properties. Clioquinol, 5-chloro-7-iodo-8-hydroxy-quinoline, was produced as a topical antiseptic and marketed as an oral intestinal amebicide as early as the 1930s.[14] It has good in vivo properties, including oral bioavailability, single-dose concentrations are dose-related, and the drug half-life in humans is 11−14 h.[14,15] In addition, clioquinol treatment has been successfully used to improve the diseased state of Alzheimer patients in a pilot phase 2 clinical trial.[16] When clioquinol (**58**) was tested for in vitro inhibitory activity toward BoNT/A LC, it exhibited moderate inhibition with an IC_{50} value of 20.3 μM (Table 2), notably improved inhibition compared to the activity of 8-hydroxy-quinoline (**54**; IC_{50} > 30 μM). Similarly, chloroxine, 5,7-dichloro-8-hydroxy-quinoline (**60**), a clinically approved antibacterial drug used in shampoos for dandruff and seborrheic dermatitis, showed moderate inhibition of BoNT/A

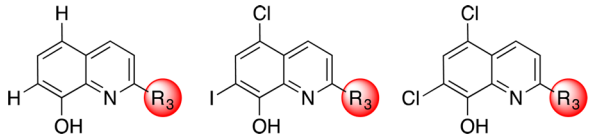

Figure 2. Structure of 8-hydroxy-quinoline (**54**; left) and the derivatives clioquinol (**58**; center) and chloroxine (**60**; right); the parent compounds have R_3 = H in each case. Methyl substitutions at R_3 increased compound inhibitory activity compared to the parent molecules.

Table 2. Substructure Analysis of the Quinolinol Scaffold

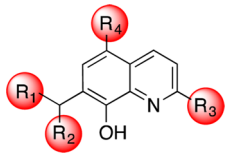

Compound	R_1	R_2	R_3	R_4	IC_{50} (μM)
54	H		H	H	>30
55	H		CH_3	H	>30
56	H		H	H	26.7 ± 3.4
57			H	H	2.2 ± 0.4
58	I		H	Cl	20.3 ± 1.6
59	I		CH_3	Cl	14.1 ± 0.7
60	Cl		H	Cl	11.5 ± 0.9
61	Cl		CH_3	Cl	10.1 ± 0.8

dx.doi.org/10.1021/jm4012164 | J. Med. Chem. 2014, 57, 669−676

Table 3. In Vitro ADME Properties of Selected Quinolinol BoNT/A LC Inhibitors

	metabolic stability, human		plasma stability, human		metabolic stability, rat		plasma stability, rat		aqueous solubility	
compd	metabolic rate (μM/min·mg)	half-life (min)	half-life (hr)	% remaining at 3 h	metabolic rate (μM/min·mg)	half-life (min)	half-life (hr)	% remaining at 3 h	pH 6.8 (nM)	pH 1.0 (μM)
34	0.215	25.5	24.4	90.9	0.130	42.2	51.1	100	74.1	1049
35	0.047	116	42.0	92.2	0.271	20.3	109	98.5	65.9	997
36	0.242	22.7	6.1	53.4	0.487	11.3	5.0	42.2	5.3	102
37	0.324	17.0	10.7	66.2	0.627	8.8	5.0	86.6	33.8	76.7
56	0.203	27.1	14.2	96.1	0.149	36.8	12.9	76.3	111	1144
57	0.186	29.6	11.4	78.7	0.637	8.6	13.5	67.3	78.0	1174
58	0.086	63.9	42.4	100	0.071	76.9	136	83.9	<1.0	38.1
60	0.112	48.9	18.6	100	0.100	55.0	67.7	100	532	326
61	0.190	28.8	24.5	92.2	0.142	38.6	115	96.9	394	1098

LC with even more potent IC_{50} of 11.5 μM relative to clioquinol (Table 2).

We next questioned if the SAR trends observed in our screening set would hold true with clioquinol and chloroxine. Interestingly, simple 2-methyl substitutions of clioquinol and chloroxine significantly improved inhibitory activities of both compounds (Table 2). 2-Methyl-clioquinol (**59**) showed a 31% improvement in potency (IC_{50} = 14.1 μM) when compared to the unmethylated clioquinol (**58**), whereas 2-methyl-chloroxine (i.e., 2-methyl-5,7-dichloro-8-hydroxy-quinoline; **61**) showed a moderate improvement of 12% (IC_{50} = 10.1 μM) when compared to the unmethylated chloroxine (**60**), confirming the observed trend with previously examined quinolinol compound pairs (Tables 1 and 2). While these are not as potent as many of the hydroxamate leads, it should be pointed out that the improved IC_{50} values of the methylated analogues of clioquinol and chloroxine (**59** and **61**) are comparable to the observed EC_{50} values of quinolinol compounds tested in a cell-based BoNT/A neurotoxicity assay.[8] Thus, although these methylated analogues have lower activity, they still may be potent enough to inhibit intracellular toxin function in cell-based models. Moreover, benzimidazole acrylonitrile-based[17] and D-cysteine-based[18] inhibitor concentrations required to exhibit 50% protection in cellular assays have been shown to be around 30 μM, concentrations similar to the IC_{50} values of clioquinol and chloroxine (**58** and **60**). Collectively, these data suggest that the two existing drugs with extensive pharmacokinetic and pharmacodynamic data and detailed toxicity profiles could be repurposed for further cellular and in vivo testing as well as serve as an attractive template for developing more potent BoNT/A LC inhibitors with superior in vivo properties to those of the existing BoNT/A LC inhibitors.

Our previous studies have shown that incorporation of drug metabolism and pharmacokinetic filters during the early phase of BoNT/A LC drug discovery process is crucial in prioritizing compounds and advancing only viable leads into the mouse bioassay and preclinical development.[4] Existing BoNT/A LC small molecule inhibitors tend to display poor water solubility, high cytotoxicity, low cell permeability, and/or low in vivo half-life and are found ineffective only once progressed to in vivo studies.[5] The cytotoxicity of quinolinol compounds has been evaluated by Roxas-Duncan et al., who observed no cytotoxicity when quinolinol compounds were tested in a Neuro-2a-based cellular model at concentrations up to 50 μM, implying this pharmacological parameter should not prevent their use in cellular or in vivo assays.[8]

Nine compounds, including clioquinol and chloroxine, were selected based on their initial in vitro potency, absence of known reactive groups, and availability of compound pairs with or without the R_3 methyl group, and advanced into a set of in vitro ADME assays including aqueous solubility, metabolic stability in human and rat liver microsomes, and human and rat plasma stability (Table 3). These assays were selected as they directly affect formulation and in vivo exposure, respectively. Moreover, compounds were assayed in the context of human and mouse liver microsomal and plasma metabolic stability, due to potential species differences in liver and plasma metabolism, as well as to inform future toxicology and clinical studies designs.

Aqueous solubility of the nine quinolinol inhibitors was determined at two different pH values to evaluate the feasibility of oral administration in possible in vivo assays and preclinical studies (Table 3). All compounds exhibited extremely low aqueous solubility at pH 6.8, ranging between <1 nM (**58**) and 0.5 μM (**60**), concentrations that are well below their IC_{50} values, suggesting none of the compounds would be soluble in the environment of the small intestine. However, when the pH was reduced to 1.0, compound solubility markedly increased, ranging between 38 μM (**58**) to almost 1.2 mM (**57**), suggesting that quinolinol compounds may be amenable to oral dosing paradigms.[19] This finding is in agreement with oral dosing as the preferred route of administration of clioquinol, where serum levels of clioquinol in patients with Alzheimer's disease ranged between 13 to 25 μM at total oral daily dosages of 250 to 750 mg that were well below the dose associated with neurological toxicity (20−30 mg/kg/day).[14,15]

In general, all of the compounds, with the exception of compound **36**, were highly stable in human and rat plasma, with stability $t_{1/2}$ in plasma averaging 23.5 ± 4.5 h for human and 63.8 ± 18.2 h for rat plasma, respectively. All of the compounds tested, save compounds **35** and **58**, showed high metabolic rates both in human as well as in rat liver microsomes. Consequently, the half-lives of the compounds in either species did not exceed 60 min, with the exception of compounds **35** (human $t_{1/2}$ = 116 min) and **58** (human $t_{1/2}$ = 64 min, rat $t_{1/2}$ = 77 min), which is comparable to the published half-lives of hydroxamate-based BoNT/A LC inhibitors.[4]

The results of this study indicate that 8-hydroxy-quinoline compounds represent an attractive scaffold for design of potent BoNT/A LC inhibitors. A screen of 188 quinolinol compounds from commercially available small molecule repositories against recombinant BoNT/A LC showed that a broad range of substitutions is well tolerated by the enzyme, further validating

dx.doi.org/10.1021/jm4012164 | J. Med. Chem. 2014, 57, 669−676

the hypothesis that BoNT/A LC flexibility can significantly impact small molecule inhibitor design. Indeed, flexibility of BoNT/A LC substrate binding site has previously been suggested by X-ray crystallography[10,20,21] and implied in our data through observed inconsistency in SAR trend across hydroxamate compound series.[7] However, the inhibitory profile of two clinically approved molecules with established pharmacokinetics, clioquinol and chloroxine, demonstrated that these compounds could be repurposed for BoNT/A testing and may serve as a scaffold for future design and optimization. The most potent compound from our screen (**4**) displayed a submicromolar IC_{50}, which is the most potent inhibition of BoNT/A LC by a quinolinol lead. Despite the poor solubility of the entire series of compounds at pH 6.8, improved solubility at pH 1.0 argues for testing in oral dosing models to enhance in vivo exposure. Presently, pharmacokinetic analysis of these compounds is currently underway and will be reported in due course.

EXPERIMENTAL PROCEDURES

Materials. 8-Hydroxy-quinoline (**54**; cat. no. 252565, 99% purity), 2-methyl-8-hydroxy-quinoline (**55**; cat. no. H57602, 98% purity), 5,7-dichloro-2-methyl-8-hydroxy-quinoline (**61**; cat. no. 130532, 98% purity), and 5-chloro-7-iodo-2-methyl-8-hydroxy-quinoline (**59**; cat. no. PH004692) were purchased from Sigma-Aldrich, 5-chloro-7-iodo-8-hydroxy-quinoline (**58**; cat. no. A11137, 98% purity) was purchased from Alfa Aesar, 5,7-dichloro-8-hydroxy-quinoline (**60**; cat. no. 11343, 99% purity) was obtained from Acros Organics. All ChemBridge compounds were certified to have met the high quality standard of 100% NMR identification and had a purity level of at least 90%. Purity of ChemDiv compounds was confirmed by the supplier by LC/MS and NMR and had a purity of >95%. All synthesized compounds assayed for enzyme activity were purified by semipreparative reversed phase HPLC and found to be greater than 95% pure based on analysis by 300 MHz ^{1}H NMR and analytical scale reversed phase HPLC with diode array detection.

General Procedures. LC/MS data were determined with a Waters Alliance 2695 HPLC/MS (Waters Symmetry C18, 4.6 × 75 mm, 3.5 μm) with a 2996 diode array detector from 210−400 nm; the solvent system is 5−95% MeCN in water (with 0.1% TFA) over nine minutes using a linear gradient, and retention times are in minutes. Mass spectrometry was performed on a Waters ZQ using electrospray in positive mode. Preparative reversed phase HPLC was performed on a Waters Sunfire column (19 × 50 mm, C18, 5 μm) with a 10 min mobile phase gradient of 10% acetonitrile/water to 90% acetonitrile/water with 0.1% TFA as buffer using 214 and 254 nm as detection wavelengths. Injection and fraction collection were performed with a Gilson 215 liquid handling apparatus using Trilution LC software.

7-(((Pyridin-2-yl)amino)methyl)quinolin-8-ol (56). To a solution of 2-aminopyridine (33 mg, 0.35 mmol) and 8-hydroxyquinoline-7-aldehyde (50 mg, 0.29 mmol) in dichloromethane (3 mL) was added sodium triacetoxyborohydride (74 mg, 0.34 mmol) and the mixture was stirred for 4 days. The solvent was evaporated and the residue was dissolved in methanol and water and purified by preparative reversed phase HPLC (see general procedures). The product fractions were combined, diluted with ethyl acetate (50 mL), and washed with saturated sodium bicarbonate solution (25 mL) and brine (25 mL). The organic layer was dried (Na_2SO_4) and evaporated to leave the product as a light yellow solid (25 mg, 34%). ^{1}H NMR (300 MHz, $CDCl_3$) δ 8.80 (dd, J = 4.1 Hz, J = 1.4 Hz, 1H), 8.43 (dd, J = 8.6 Hz, J = 1.5 Hz, 1H), 8.17 (dd, J = 5.0 Hz, J = 1.1 Hz, 1H), 7.55−7.40 (m, 3H), 7.11 (dd, J = 8.2 Hz, J = 2.6 Hz, 1H), 6.63 (ddd, J = 6.5 Hz, J = 5.3 Hz, J = 4.4 Hz, 1H), 6.42 (d, J = 8.2 Hz, 1H), 4.85 (d, J = 5.3 Hz, 2H), 4.13 (bs, 1H); ESI MS $(M + H)^+$ = 252; HPLC R_t = 1.27 min.

7-(Phenyl((pyridin-2-yl)amino)methyl)quinolin-8-ol (57). To a solution of benzaldehyde (24 mg, 0.23 mmol, 23 μL) and 2-aminopyridine (22 mg, 0.23 mmol) in 95% ethanol (1 mL) was added 8-hydroxyquinoline (34 mg, 0.23 mmol) and the mixture stirred for 7 days. The reaction mixture was diluted with water (0.15 mL) and purified by reversed phase HPLC (see general procedures). The major product fractions were combined, diluted with ethyl acetate (20 mL), washed with saturated sodium bicarbonate solution (25 mL) and brine (25 mL). The organic layer was dried (Na_2SO_4) and evaporated to leave a beige solid (25 mg, 33%). ^{1}H NMR (300 MHz, $CDCl_3$) δ 8.77 (dd, J = 4.4 Hz, J = 1.7 Hz, 1H), 8.11 (dd, J = 8.2 Hz, J = 1.5 Hz, 1H), 8.09 (bs, 1H), 7.57 (d, J = 8.8 Hz, 1H), 7.50−7.20 (m, 9H), 6.57 (ddd, J = 7.0 Hz, J = 5.0 Hz, J = 1.0 Hz, 1H), 6.43 (d, J = 6.4 Hz, 1H), 6.41 (d, J = 8.5 Hz, 1H), 5.60 (bd, J = 5.3 Hz, 1H); ESI MS $(M + H)^+$ = 328; HPLC R_t = 3.04 min.

SNAPtide Assay. Inhibitory activity of small molecules from the compound libraries was determined by the decrease in BoNT/A LC enzymatic activity toward the SNAPtide fluorogenic substrate (List Biological Laboratories). The assay was performed in 40 mM Hepes, pH 7.4, 0.01% Tween-20 at room temperature (22 °C). In dose−response IC_{50} assays, 9 point 1:3 dilutions of compounds in DMSO (1 μL) were preincubated with 10 μL of 70 nM BoNT/A LC (expressed in *Escherichia coli* and purified as described elsewhere[22]) in 79 μL of 40 mM Hepes buffer in a 96-well black plate (Greiner) for 5 min at room temperature. Subsequently, 10 μL of 7 μM SNAPtide were added to initiate the reaction. The final concentration of DMSO was 2%. Fluorescence was recorded continuously for 105 min at room temperature on a Synergy MX plate reader (BioTek) with excitation at 490 nm and emission at 523 nm. Enzyme velocities used for determination of IC_{50} values were calculated from the linear portion of the response curve.

In Vitro Microsomal Stability. Metabolic stability of lead compounds was assessed in vitro by the method of Ackley et al.[23] Briefly, liver microsome preparations (BD Genetest Products and Services, Woburn, MA) were isolated from humans (pooled from 10 male donors) or Sprague−Dawley rats (male rats, 8−10 weeks of age). Assays were conducted using 0.125 mg/mL protein concentration (total protein concentration in the microsomal solution) and 1.0 μM drug concentration under incubation conditions of 37 °C. Metabolic stability was determined following 0, 5, 15, 30, and 60 min of incubation time. The samples were analyzed by reversed phase LC using a triple quadrupole mass spectrometer. Compound specific transitions of parent ion to product ion were monitored and percent remaining calculated based on peak area of 15−60 min time points (relative to time zero). Half-life calculations were determined using the formula $t_{1/2} = -\ln(2)/k$, where k (min^{-1}) is the turnover rate constant (the slope) estimated from a log−linear regression of the percentage compound remaining versus time.

Plasma Stability. Percent remaining of compound of interest was determined in plasma (Valley Biomedical, Winchester, VA) at an analyte concentration of 1.0 μM following incubation at 37 °C according to the published protocol.[24] Time points were taken at 0, 1, 3, 5, and 24 h, precipitating plasma proteins with internal standard in cold acetonitrile. Samples were analyzed by LC−MS/MS and half-life was calculated following regression analysis.

Aqueous Solubility. Aqueous solubility was determined by the method of Zhou et al. using a miniaturized shake flask approach at pH 1.0 and 6.8 and an analyte concentration of 1.0 mM.[25] Aqueous solutions of analyte were incubated at room temperature in the chamber of a Whatman (Piscataway, NJ) Mini-UniPrep syringeless filter for 24 h while shaking gently (600 rpm). Subsequent to incubation, filter plungers were pushed down to the bottom of the syringeless filter chamber assemblies, allowing filtrate to enter the plunger compartment. Following an additional 30 min incubation at room temperature, filtrates were diluted with 50:50 acetonitrile/water + 0.1% formic acid and analyzed by LC−MS/MS. Analyte concentrations were determined by the interpolation of peak area ratio from a calibration curve formed by matrix spiked with authentic reference material, over a calibration range of 0.05−12.5 μM (pH 6.8) or 5.0−25000 μM (pH 1.0).

LC−MS/MS Analysis. LC−MS/MS analysis was conducted using an Agilent (Santa Clara, CA) 6460 triple quadrupole mass

dx.doi.org/10.1021/jm4012164 | J. Med. Chem. 2014, 57, 669−676

spectrometer coupled with an Agilent liquid chromatography (LC) system. The LC system consists of a binary pump, degasser, column heater, and autosampler. Chromatographic separation was performed on a Waters XBridge C18 (3.5 μm, 3.0 × 50 mm) or an Agilent Zorbax SB-Aq (4.6 × 50 mm) analytical column using a ballistic gradient of mobile phase consisting of 0.1% formic acid in water (A) and 0.1% formic acid in acetonitrile (B) at a flow rate of 1.0 mL/min. Mobile phase was heated to a temperature of 45 °C.

■ ASSOCIATED CONTENT

Supporting Information

Inhibitory activities of additional 8-hydroxy-quinolines; structures of compound **57** and its inactive analogue. This material is available free of charge via the Internet at http://pubs.acs.org.

■ AUTHOR INFORMATION

Corresponding Author

*(T.J.D.) Phone: +1 (858) 784-2522. E-mail: tobin@scripps.edu.

Notes

The authors declare no competing financial interest.

■ ACKNOWLEDGMENTS

This work was supported by the National Institutes of Health (AI082190 to T.J.D.). M.C.K. was supported by an internship from the California Institute for Regenerative Medicine (TB1-01186).

■ ABBREVIATIONS USED

BoNT, botulinum neurotoxin; LC, light chain metalloprotease; SAR, structure−activity relationship; ADME, absorption, distribution, metabolism, excretion

■ REFERENCES

(1) Schantz, E. J.; Johnson, E. A. Properties and use of botulinum toxin and other microbial neurotoxins in medicine. *Microbiol. Rev.* **1992**, *56*, 80−99.

(2) Dickerson, T. J.; Janda, K. D. The use of small molecules to investigate molecular mechanisms and therapeutic targets for treatment of botulinum neurotoxin A intoxication. *ACS Chem. Biol.* **2006**, *1*, 359−369.

(3) Willis, B.; Eubanks, L. M.; Dickerson, T. J.; Janda, K. D. The strange case of the botulinum neurotoxin: using chemistry and biology to modulate the most deadly poison. *Angew. Chem., Int. Ed.* **2008**, *47*, 8360−8379.

(4) Capek, P.; Zhang, Y.; Barlow, D. J.; Houseknecht, K. L.; Smith, G. R.; Dickerson, T. J. Enhancing the Pharmacokinetic Properties of Botulinum Neurotoxin Serotype A Protease Inhibitors Through Rational Design. *ACS Chem. Neurosci.* **2011**, *2*, 288−293.

(5) Eubanks, L. M.; Hixon, M. S.; Jin, W.; Hong, S.; Clancy, C. M.; Tepp, W. H.; Baldwin, M. R.; Malizio, C. J.; Goodnough, M. C.; Barbieri, J. T.; Johnson, E. A.; Boger, D. L.; Dickerson, T. J.; Janda, K. D. An in vitro and in vivo disconnect uncovered through high-throughput identification of botulinum neurotoxin A antagonists. *Proc. Natl. Acad. Sci. U.S.A.* **2007**, *104*, 2602−2607.

(6) Boldt, G. E.; Kennedy, J. P.; Janda, K. D. Identification of a potent botulinum neurotoxin a protease inhibitor using in situ lead identification chemistry. *Org. Lett.* **2006**, *8*, 1729−1732.

(7) Smith, G. R.; Caglič, D.; Čapek, P.; Zhang, Y.; Godbole, S.; Reitz, A. B.; Dickerson, T. J. Reexamining hydroxamate inhibitors of botulinum neurotoxin serotype A: extending towards the beta-exosite. *Bioorg. Med. Chem. Lett.* **2012**, *22*, 3754−3757.

(8) Roxas-Duncan, V.; Enyedy, I.; Montgomery, V. A.; Eccard, V. S.; Carrington, M. A.; Lai, H.; Gul, N.; Yang, D. C.; Smith, L. A. Identification and biochemical characterization of small-molecule inhibitors of Clostridium botulinum neurotoxin serotype A. *Antimicrob. Agents Chemother.* **2009**, *53*, 3478−3486.

(9) Lai, H.; Feng, M.; Roxas-Duncan, V.; Dakshanamurthy, S.; Smith, L. A.; Yang, D. C. Quinolinol and peptide inhibitors of zinc protease in botulinum neurotoxin A: effects of zinc ion and peptides on inhibition. *Arch. Biochem. Biophys.* **2009**, *491*, 75−84.

(10) Silvaggi, N. R.; Boldt, G. E.; Hixon, M. S.; Kennedy, J. P.; Tzipori, S.; Janda, K. D.; Allen, K. N. Structures of clostridium botulinum neurotoxin serotype A light chain complexed with small-molecule inhibitors highlight active-site flexibility. *Chem. Biol.* **2007**, *14*, 533−542.

(11) Caglic, D.; Bompani, K. M.; Krutein, M. C.; Capek, P.; Dickerson, T. J. A high-throughput-compatible FRET-based platform for identification and characterization of botulinum neurotoxin light chain modulators. *J. Visualized Exp.* **2013**, e50908 DOI: 10.3791/50908.

(12) Capkova, K.; Salzameda, N. T.; Janda, K. D. Investigations into small molecule non-peptidic inhibitors of the botulinum neurotoxins. *Toxicon* **2009**, *54*, 575−582.

(13) Zhang, J. H.; Chung, T. D.; Oldenburg, K. R. A simple statistical parameter for use in evaluation and validation of high throughput screening assays. *J. Biomol. Screening* **1999**, *4*, 67−73.

(14) Bareggi, S. R.; Cornelli, U. Clioquinol: review of its mechanisms of action and clinical uses in neurodegenerative disorders. *CNS Neurosci. Ther.* **2012**, *18*, 41−46.

(15) Mao, X.; Schimmer, A. D. The toxicology of clioquinol. *Toxicol. Lett.* **2008**, *182*, 1−6.

(16) Ritchie, C. W.; Bush, A. I.; Mackinnon, A.; Macfarlane, S.; Mastwyk, M.; MacGregor, L.; Kiers, L.; Cherny, R.; Li, Q. X.; Tammer, A.; Carrington, D.; Mavros, C.; Volitakis, I.; Xilinas, M.; Ames, D.; Davis, S.; Beyreuther, K.; Tanzi, R. E.; Masters, C. L. Metal−protein attenuation with iodochlorhydroxyquin (clioquinol) targeting Abeta amyloid deposition and toxicity in Alzheimer disease: a pilot phase 2 clinical trial. *Arch. Neurol.* **2003**, *60*, 1685−1691.

(17) Li, B.; Cardinale, S. C.; Butler, M. M.; Pai, R.; Nuss, J. E.; Peet, N. P.; Bavari, S.; Bowlin, T. L. Time-dependent botulinum neurotoxin serotype A metalloprotease inhibitors. *Bioorg. Med. Chem.* **2011**, *19*, 7338−7348.

(18) Boldt, G. E.; Eubanks, L. M.; Janda, K. D. Identification of a botulinum neurotoxin A protease inhibitor displaying efficacy in a cellular model. *Chem. Commun.* **2006**, 3063−3065.

(19) Reichman, M.; Gill, H. Automated Drug Sceening for ADMET Properties. In *Drug Metabolism Handbook: Concepts and Applications*; Nassar, A. F., Hollenberg, P. F., Scatina, J., Eds.; John Wiley & Sons, Inc.: Hoboken, NJ, 2009; p 137.

(20) Burnett, J. C.; Schmidt, J. J.; McGrath, C. F.; Nguyen, T. L.; Hermone, A. R.; Panchal, R. G.; Vennerstrom, J. L.; Kodukula, K.; Zaharevitz, D. W.; Gussio, R.; Bavari, S. Conformational sampling of the botulinum neurotoxin serotype A light chain: implications for inhibitor binding. *Bioorg. Med. Chem.* **2005**, *13*, 333−341.

(21) Thompson, A. A.; Jiao, G. S.; Kim, S.; Thai, A.; Cregar-Hernandez, L.; Margosiak, S. A.; Johnson, A. T.; Han, G. W.; O'Malley, S.; Stevens, R. C. Structural characterization of three novel hydroxamate-based zinc chelating inhibitors of the Clostridium botulinum serotype A neurotoxin light chain metalloprotease reveals a compact binding site resulting from 60/70 loop flexibility. *Biochemistry* **2011**, *50*, 4019−4028.

(22) Baldwin, M. R.; Bradshaw, M.; Johnson, E. A.; Barbieri, J. T. The C-terminus of botulinum neurotoxin type A light chain contributes to solubility, catalysis, and stability. *Protein Expression Purif.* **2004**, *37*, 187−195.

(23) Ackley, D. C.; Rockich, K. T.; Baker, T. R. In Vitro Methods. In *Optimization in Drug Discovery*; Yan, Z., Caldwell, G. W., Eds. Humana Press: Totowa, NJ., 2004; p 151.

(24) Di, L.; Kerns, E. H.; Hong, Y.; Chen, H. Development and application of high throughput plasma stability assay for drug discovery. *Int. J. Pharm.* **2005**, *297*, 110−119.

(25) Zhou, L.; Yang, L.; Tilton, S.; Wang, J. Development of a high throughput equilibrium solubility assay using miniaturized shake-flask method in early drug discovery. *J. Pharm. Sci.* **2007**, *96*, 3052−3071.